INTEGRATED THERMAL ENERGY STORAGE IN GRAPHENE-BASED COMPOSITE EVAPORATOR FOR HIGH-EFFICIENCY WATER GENERATION

Kit-Ying Chan[1], Xiaomeng Zhao[1], Xiuli Dong[1], Ling Liu[1] and Xi Shen[1*]
[1] Department of Aeronautical and Aviation Engineering, The Hong Kong Polytechnic University, Hong Kong SAR, China
* Corresponding author (xi.shen@polyu.edu.hk)

Keywords: *Graphene composite, thermal energy storage, hydrogels, and water evaporation*

ABSTRACT

Solar-driven water evaporation is a promising approach to ease the problem of global water shortages using sustainable energy. Numerous research works have been focused on the development and optimization of solar absorbers to achieve highly efficient interfacial solar vapor generation. However, it remains a great challenge to achieve high-performance water generation due to the intermittent solar irradiation. Herein, an integrated structure consisting of graphene microlattice (GML) filled with carbon nanotubes (CNT) reinforced phase change material (PCM) for thermal energy storage and graphene oxide (GO)-based hydrogel for water evaporation was developed to extend the duration of water generation. The CNT-GML/PCM composite not only acts as an additional heat source under solar irradiation, achieving a high evaporation rate of 3.55 kg/m^2 h under one sun, but also releases latent heat to the hydrogel evaporator when the solar illumination was turned off, maintaining a high evaporation rate of 2.67 kg/m^2 h for 30 minutes. This value is even higher than the evaporation rate of GO-based hydrogel evaporator, which is 2.08 kg/m^2 h under one sun. During three 60-minute on and 30-minute off cycles, the total water generation of the integrated structure reached to 14.64 kg/m^2, which is almost a double of the hydrogel evaporator only (7.39 kg/m^2), thanks to the additional heat supply from CNT-GML/PCM composites. This work demonstrates an effective strategy to prolong the duration of water generation under practical intermittent sunlight conditions by integrating thermal energy storage capability into solar evaporators.

1 INTRODUCTION

Solar-driven water evaporation plays a critical role in freshwater generation by harvesting solar energy and converting it to heat using light-absorbing evaporators consist of nanofillers such as graphene oxide (GO) [1, 2], carbon nanotubes (CNT) [3-5] and MXene [6, 7]. In the past decade, myriad research efforts have been devoted to engineering the solar evaporators for broadband solar absorption, reduced heat losses, and efficient water supply for high-performance water evaporation [8]. In particular, constructing three-dimensional (3D), highly porous microstructures of nanocomposite evaporators have been demonstrated as an effective approach to achieve excellent thermal management, fast water transport and high sunlight absorption simultaneously, leading to a high evaporation rate of ~2 kg/m^2 h [6, 9-11]. Recently, hydrogel-based evaporators, such as hydrophilic polyvinyl alcohol (PVA) hydrogels, with superior evaporation rate (>3.0 kg/m^2 h) have been developed by exploiting the abundant hydroxyl groups (-OH) in polymer networks. The strong interaction between hydrophilic polymer chains and water molecules can form layers of intermediate water, which have lower evaporation enthalpy than free water [12-14]. As such, less energy is needed for hydrogel evaporators to generate the same amount of water when compared to conventional ones. Although the performance of water evaporation has been significantly improved by tailoring the composition and microstructure of evaporators, it is still very challenging to translate the evaporators from laboratory standards to practical freshwater production due to the intermittent sunlight conditions in practice. Therefore, it is highly desirable to develop an advanced solar-driven evaporation system that can overcome the challenges caused by intermittent solar irradiation.

Recently, interfacial evaporators using phase change material (PCM) microcapsules as both solar absorbers and thermal energy storage have been developed [15, 16]. The PCM microcapsule-based

evaporation systems exhibited high evaporation rates of ≥2 kg/m^2 h under one sun. The presence of PCM microcapsules also maintained a high evaporation rate during the light on/off cycles, demonstrating continued evaporation performance due to the intermittence of solar irradiation. However, the microcapsules were separated by a cotton pad for water supply and thus were not interconnected, leading to limited contact areas between microcapsules and a low thermal conductivity of the interfacial evaporation layer despite their broadband light absorption and high photothermal conversion. As such, the heat absorbed by the microcapsules on the top layer might not be effectively transferred to and stored in the microcapsules underneath, limiting the thermal energy storage efficiency and water evaporation rate. In addition to PCM microcapsules, paraffin block was also integrated into polypyrrole (PPy)-based evaporator to enhance the evaporation performance under intermittent solar irradiation [17]. Similarly, the low thermal conductivity of paraffin block without thermally conductive network also restricted the thermal energy storage performance of the integrated device. So far, the rational design of advanced evaporation systems by integrating thermal storage composite to solar evaporators is still a very challenging task. Besides, there lacks a clear guideline for more effective evaluation and comparison of the thermal storage efficiency for all-weather freshwater generation of those advanced systems reported previously.

Herein, we aim to develop an integrated evaporation system with both high thermal energy storage and water evaporation performance to extend the duration of freshwater generation, as shown in Fig. 1. Highly connected graphene microlattice (GML) filled with PCM was used for thermal storage. Carbon nanotubes (CNTs) were added into the PCM to form additional thermally conductive network for improved thermal storage efficiency and enhanced solar absorption. A novel plate freeze-casting technique was also developed to produce graphene oxide (GO) reinforced PVA hydrogels with pore channels in radiating pattern for balanced thermal management and gradient pore size for high water transport. Under solar irradiation, the CNT-GML/PCM composite functioned as an additional heat source to GO/PVA hydrogel evaporator, achieving a high evaporation rate of 3.55 kg/m^2 h under one sun. Surprisingly, the integrated device maintained an evaporation rate of 2.67 kg/m^2 h for 30 minutes when the solar illumination was turned off, thanks to the latent heat released from the CNT-GML/PCM composite. The total water generation of the integrated structure for three consecutive light-on (60 minutes) and light-off (30 minutes) cycles reached to 14.64 kg/m^2, twice as high as that of the hydrogel evaporator (7.39 kg/m^2). This work presented an effective strategy to prolong the duration of water generation under practical intermittent sunlight conditions by integrating thermal energy storage capability into solar evaporators.

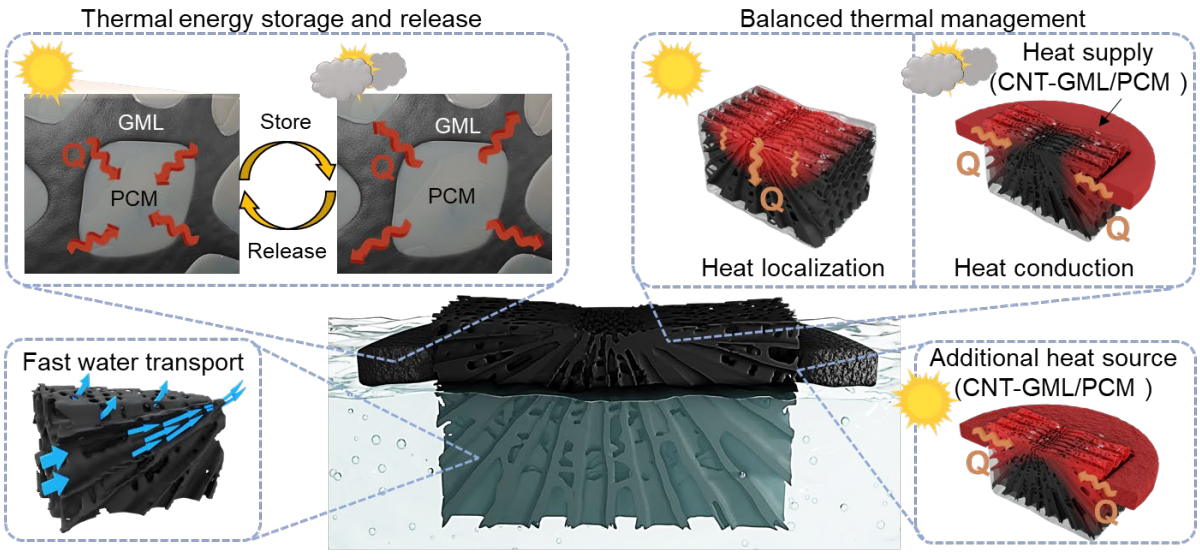

Fig 1. Rational design of solar-driven evaporation system for all-weather freshwater generation.

2 METHODOLOGY

2.1 FABRICATION OF THERMAL STORAGE COMPONENT

3D graphene structures were fabricated on Ni microlattice template by chemical vapor deposition (CVD) [18]. After the etching of the Ni template, a free-standing GML with pore size of several hundred micrometers was obtained. Paraffin wax used as PCM was melted at 70°C and mixed with 5wt% CNTs for enhanced thermal conductivity and solar absorption. Then, the CNT/PCM mixture was infiltrated into the 3D structure under vacuum condition. The center of solidified CNT-GML/PCM composite was cut and assembled into an integrated device.

2.2 FABRICATION OF EVPORATION COMPONENT AND THE INTEGRATED DEVICE

A PVA solution was obtained by dissolving PVA powders in deionized (DI) water at 90°C with stirring for 2 hours. The PVA solution was then mixed with a GO solution under vigorous stirring for 30 min, followed by a plate freeze-casting technique, as shown in Fig. 2a. The ice crystals grew in a radiating pattern from the center cold source to various points on the edges. The frozen sample was placed in a freezer at -40°C overnight to allow the completion of physicochemical crosslinking, followed by thawing at ambient to obtain a GO/PVA hydrogel. Afterward, the hydrogel was placed at the center of CNT-GML/PCM composite to form an integrated device (Fig. 1).

2.3 CHARACTERIZATIONS

The microstructures of GO/PVA hydrogels and CNT-GML/PCM composites were characterized by a scanning electron microscopy (SEM, Hitachi TM3030). The solar absorption was calculated by $\alpha = 1 - R - T$, where R is the reflectance and T is the transmittance of samples. Both R and T were determined using an ultraviolet (UV)-visible-near infrared (NIR) spectrometer (Perkin Elmer Lambda 950) in a wavelength range of 0.25–2.5 μm. The solar weighted absorption was calculated according to the specification, ASTM G173-03. The heat capacity of CNT-GML/PCM composites was obtained using differential scanning calorimeter (DSC, Mettler Toledo).

The solar steam generation tests were carried out using a customized setup, which consists of a solar irradiation simulator (Xenon lamp, PLS-SXE300) with a solar filter and diffuser to ensure the solar spectrum range and uniform light intensity, and an analytical balance (FA 2004) with an accuracy of 0.1 mg. The light intensity was measured using a full spectrum light power meter (PL, MW2000). The test setup was enclosed in an opaque chamber with interior temperature of 23 – 25°C and humidity of 40 – 45% under a breezeless condition. The analytical balance was connected to a computer to record the time-dependent mass change of water due to steam generation. The surface temperatures of GO/PVA hydrogels and CNT-GML/PCM composites during the solar steam tests were monitored using the thermocouples (CENTER-309 Portable Digital Thermometer).

3 RESULTS AND DISCUSSION

3.1 FABRICATION AND WATER EVAPORATION PERFORMANCE OF GO/PVA HYDROGELS

The root-like structure with unique hierarchical pore channels of GO/PVA hydrogels were produced using the plate freeze-casting technique, as shown in Fig. 2a. The radiating pattern (Fig. 2b,c) and gradient pore channels boosted water transport in the hydrogel. The presence of abundant, small pores on the evaporation surface (Fig. 2d) also offered a larger surface area for interfacial evaporation. Thanks to the highly porous structures created by freeze-casting, both GO/PVA hydrogels fabricated using plate-freezing and unidirectional-freezing exhibited the same, high solar-weighted absorption of 94% (Fig. 2e). Due to the better thermal management of root-like structure, the surface temperature of GO/PVA hydrogels fabricated using plate-freezing reached to 32°C under one sun (Fig. 2f), 2°C higher than the hydrogel produced using unidirectional-freezing. These resulted in a higher evaporation rate of the GO/PVA hydrogel fabricated using plate-freezing (2.24 kg/m^2 h) when compared to the sample fabricated using unidirectional-freezing (1.93 kg/m^2 h), as shown in Fig. 2g.

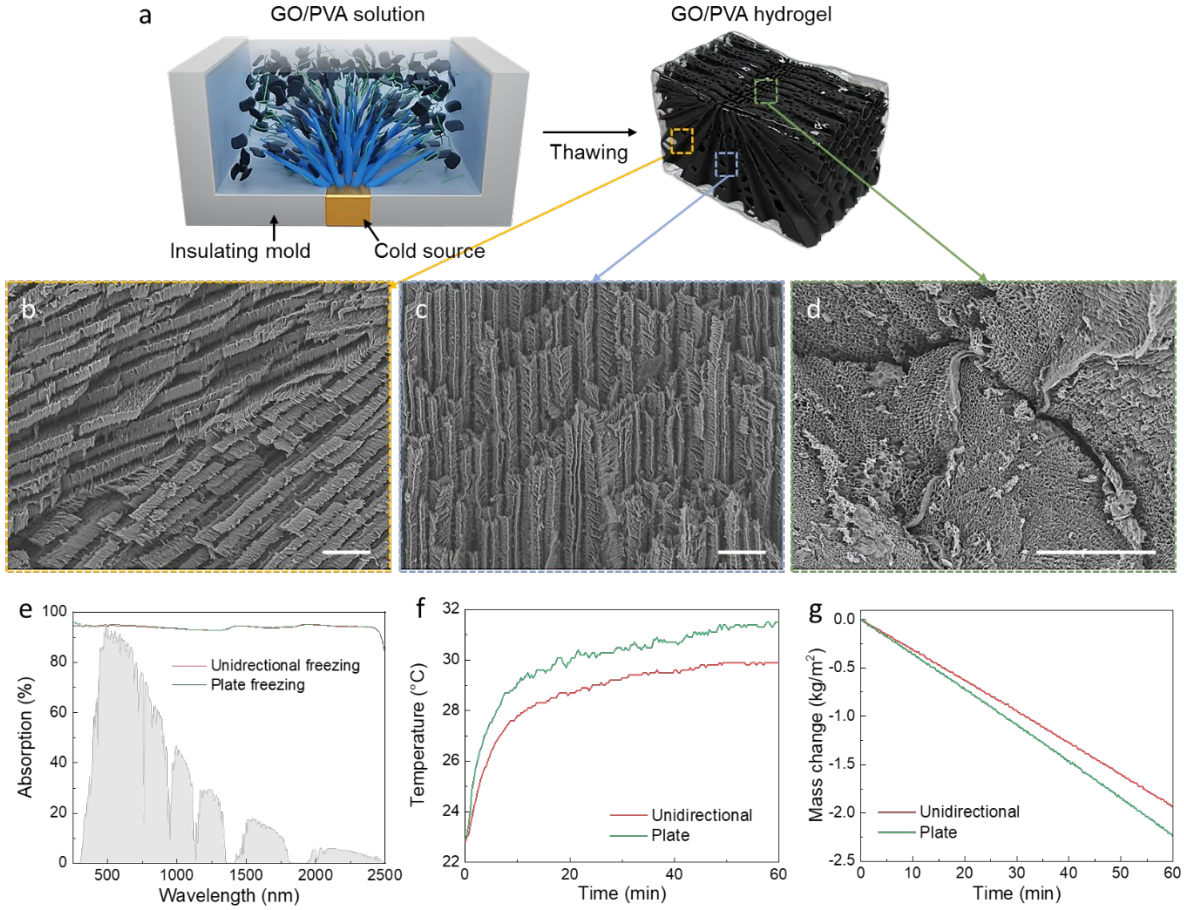

Fig. 2. Fabrication and water evaporation performance of GO/PVA hydrogels. (a) Schematics of the set-up and operating principle of the plate freeze-casting for GO/PVA hydrogels. SEM images showing (b,c) the pore channels in radiating pattern and (d) the highly porous evaporation surface. Scale bars: 100 µm. (e) Solar absorption spectra of GO/PVA hydrogels fabricated using different freeze-casting methods. (f) Surface temperatures and (g) time-dependent mass changes of GO/PVA hydrogels under one sun.

3.2 LIGHT ON/OFF CYCLES FOR THE INTEGRATED DEVICE

Since epoxy cannot store thermal energy, as shown in Fig. 3a, CNT-GML/epoxy composite was used as a control to evaluate the effect of thermal energy storage for water evaporation. Due to the high surface area of GML, the GML-based composites have abundant GML/epoxy or GML/PCM interfaces with mismatched refractive indices, promoting extensive light scattering. Together with the presence of CNT, the solar-weighted absorption of both CNT-GML/epoxy and CNT-GML/PCM composites reached to 96%, as presented in Fig. 3b. The hydrogel evaporators surrounded by these composites (Fig. 1) showed higher surface temperatures than the hydrogel alone under one sun (Fig. 3c). This could be attributed to the additional heat supply from the GML samples to the hydrogel evaporators under solar illumination. As such, the light-on evaporation rates of hydrogels equipped with CNT-GML/epoxy and CNT-GML/PCM composites are 3.20 and 3.55 kg/m^2 h respectively, as shown in Fig. 3d and 3e, both are higher than that of hydrogel only (2.08 kg/m^2 h).

Thanks to the latent heat released from the PCM after turning the light off, the cooling rate of hydrogel equipped with CNT-GML/PCM composites was significantly reduced (Fig. 3c) when compared to hydrogel only and hydrogel equipped with CNT-GML/epoxy composite, maintaining a high evaporation rate of 2.67 kg/m^2 h during the 30-minute light-off cycle. It is worthy to note that this value is even higher than the light-on evaporation rate of hydrogel only, demonstrating the effectiveness of CNT-GML/PCM composite for extending the operation duration of solar evaporators under intermittent solar irradiation. As shown in Fig. 3f, the integrated hydrogel evaporator and CNT-

GML/PCM composite exhibited both a high evaporation rate under one sun and high freshwater generation per unit solar energy input under light on/off cycles compared to the state-of-the-art solar evaporators [5-7, 14, 19-27] and integrated devices [15-17, 28]. Therefore, the rational design of the integrated device consisting of GO/PVA hydrogels and CNT-GML/PCM composites offered a promising solution for more energy-efficient water evaporation under intermittent solar irradiation.

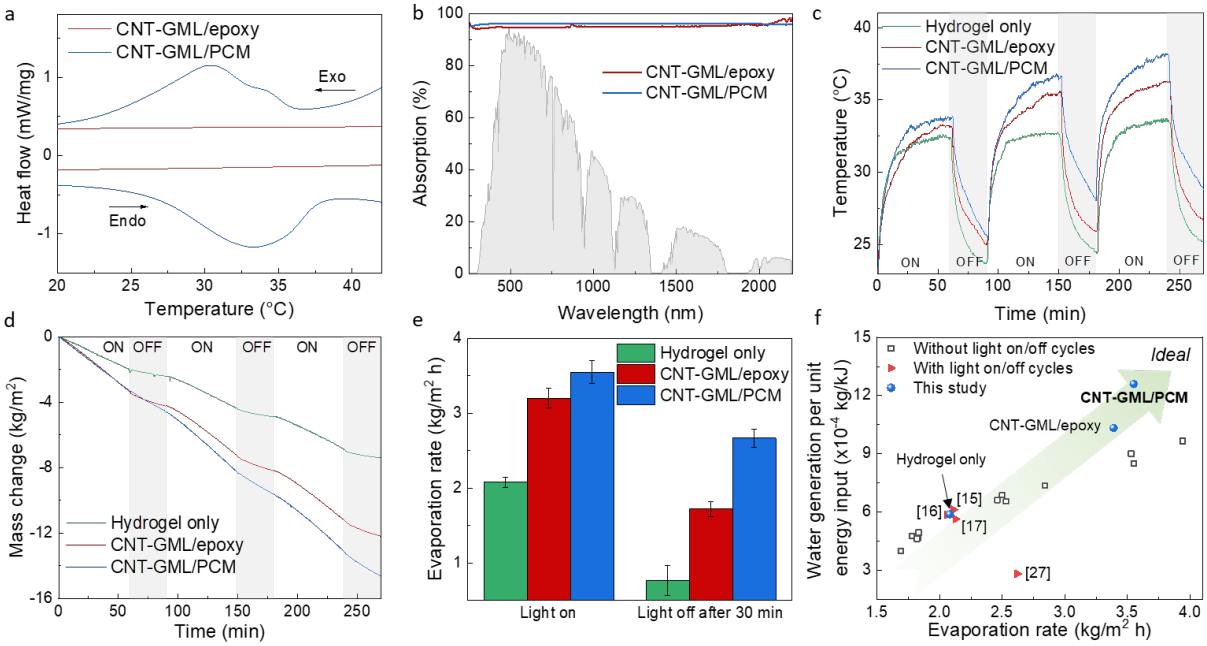

Fig. 3. Water evaporation performance of the integrated device under light on/off cycles. (a) DSC thermograms of GML samples. (b) Solar absorption spectra of GML samples. (c) Surface temperatures and (d) mass changes of hydrogel evaporators equipped with CNT-GML/epoxy and CNT-GML/PCM composites during three light on-off cycles under one sun. (e) The light-on and light-off evaporation rates averaged from three cycles. (f) Comparison of water generation per unit energy input and light-on evaporation rate under one sun with different solar evaporators [5-7, 14, 19-27] and integrated devices [15-17, 28] reported in the literature.

4 CONCLUSIONS

In summary, an integrated device consisting of GO/PVA hydrogel as solar evaporator and CNT-GML/PCM composite as thermal energy storage device was developed for highly efficient solar-powered freshwater generation. The radial pore channels and balanced thermal management of GO/PVA hydrogels contributed to a high evaporation rate of 2.24 kg/m^2 h under one sun irradiation. The CNT-GML/PCM composite functions as an additional heat supply to the hydrogel evaporator, further enhancing the light-on evaporation rate to 3.55 kg/m^2 h. During the 30-minute light-off cycle, the latent heat stored in the CNT-GML/PCM composite was released to the hydrogel evaporator to continue the water evaporation process, maintaining a high evaporation rate of 2.67 kg/m^2 h in the dark condition. This work proposed a rational design of integrating thermal energy storages into the water evaporators to prolong the operation of water generation under practical intermittent sunlight conditions.

ACKNOWLEDGEMENTS

This project was financially supported by the Research Grants Council (162007220) and the start-up fund for new recruits of PolyU (P0038855 and P0038858).

REFERENCES

[1] C. T. K. Finnerty, A. K. Menon, K. M. Conway, D. Lee, M. Nelson, J. J. Urban, D. Sedlak, and B. Mi, "Interfacial Solar Evaporation by a 3D Graphene Oxide Stalk for Highly Concentrated

Brine Treatment," *Environmental Science & Technology,* vol. 55, no. 22, pp. 15435-15445, 2021, doi: 10.1021/acs.est.1c04010.

[2] Y. Li, T. Gao, Z. Yang, C. Chen, Y. Kuang, J. Song, C. Jia, E. M. Hitz, B. Yang, and L. Hu, "Graphene oxide-based evaporator with one-dimensional water transport enabling high-efficiency solar desalination," *Nano Energy,* vol. 41, pp. 201-209, 2017, doi: 10.1016/j.nanoen.2017.09.034.

[3] P. Cao, L. Zhao, J. Zhang, L. Zhang, P. Yuan, Y. Zhang, and Q. Li, "Gradient Heating Effect Modulated by Hydrophobic/Hydrophilic Carbon Nanotube Network Structures for Ultrafast Solar Steam Generation," *ACS Appl Mater Interfaces,* vol. 13, no. 16, pp. 19109-19116, 2021, doi: 10.1021/acsami.0c21831.

[4] N. Hu, S. Zhao, T. Chen, X. Lu, and J. Zhang, "Janus Carbon Nanotube@poly(butylene adipate-co-terephthalate) Fabric for Stable and Efficient Solar-Driven Interfacial Evaporation," *ACS Appl Mater Interfaces,* vol. 14, no. 40, pp. 46010-46022, 2022, doi: 10.1021/acsami.2c11325.

[5] L. Zhao, Z. Yang, J. Wang, Y. Zhou, P. Cao, J. Zhang, P. Yuan, Y. Zhang, and Q. Li, "Boosting solar-powered interfacial water evaporation by architecting 3D interconnected polymetric network in CNT cellular structure," *J. Chem. Eng.,* vol. 451, p. 138676, 2023, doi: 10.1016/j.cej.2022.138676.

[6] H. Zhang, X. Shen, E. Kim, M. Wang, J. H. Lee, H. Chen, G. Zhang, and J. K. Kim, "Integrated Water and Thermal Managements in Bioinspired Hierarchical MXene Aerogels for Highly Efficient Solar-Powered Water Evaporation," *Adv. Funct. Mater.,* vol. 32, no. 19, p. 2111794, 2022, doi: 10.1002/adfm.202111794.

[7] B. Zhang, P. W. Wong, and A. K. An, "Photothermally enabled MXene hydrogel membrane with integrated solar-driven evaporation and photodegradation for efficient water purification," *J. Chem. Eng.,* vol. 430, p. 133054, 2022, doi: 10.1016/j.cej.2021.133054.

[8] Y. G. F Zhao, X Zhou, W Shi, G Yu, "Materials for solar-powered water evaporation," *Nat. Rev. Mater.,* vol. 5, pp. 388–401, 2020, doi: 10.1038/s41578-020-0182-4

[9] W. Xu, Y. Xing, J. Liu, H. Wu, Y. Cui, D. Li, D. Guo, C. Li, A. Liu, and H. Bai, "Efficient Water Transport and Solar Steam Generation via Radially, Hierarchically Structured Aerogels," *ACS Nano,* vol. 13, no. 7, pp. 7930-7938, 2019, doi: 10.1021/acsnano.9b02331.

[10] L. Li, N. He, B. Jiang, K. Yu, Q. Zhang, H. Zhang, D. Tang, and Y. Song, "Highly Salt-Resistant 3D Hydrogel Evaporator for Continuous Solar Desalination via Localized Crystallization," *Adv. Funct. Mater.,* vol. 31, no. 43, p. 2104380, 2021, doi: 10.1002/adfm.202104380.

[11] Y. Guo, L. S. de Vasconcelos, N. Manohar, J. Geng, K. P. Johnston, and G. Yu, "Highly Elastic Interconnected Porous Hydrogels through Self-Assembled Templating for Solar Water Purification," *Angew. Chem. Int. Ed.,* vol. 61, no. 3, p. e202114074, Jan 17 2022, doi: 10.1002/anie.202114074.

[12] Y. Guo, H. Lu, F. Zhao, X. Zhou, W. Shi, and G. Yu, "Biomass-Derived Hybrid Hydrogel Evaporators for Cost-Effective Solar Water Purification," *Adv Mater,* vol. 32, no. 11, p. e1907061, 2020, doi: 10.1002/adma.201907061.

[13] F. Z. X Zhou, Y Guo, B Rosenberger, G Yu, "Architecting highly hydratable polymer networks to tune the water state for solar water purification," *Sci. Adv.,* vol. 5, no. 6, p. eaaw5484, 2019.

[14] X. Zhou, F. Zhao, Y. Guo, Y. Zhang, and G. Yu, "A hydrogel-based antifouling solar evaporator for highly efficient water desalination," *Energy Environ. Sci.,* vol. 11, no. 8, pp. 1985-1992, 2018, doi: 10.1039/c8ee00567b.

[15] M. Zhang, K. Sun, Z. Zheng, H. Liu, and X. Wang, "Development of MXene-decorated sodium alginate/SiO2@n-docosane hierarchical phase-change microcapsules for solar-driven sustainable seawater desalination," *Desalination,* vol. 550, 2023, doi: 10.1016/j.desal.2023.116380.

[16] H. Shen, Z. Zheng, H. Liu, and X. Wang, "A solar-powered interfacial evaporation system based on MoS2-decorated magnetic phase-change microcapsules for sustainable seawater desalination," *J. Mater. Chem. A,* vol. 10, no. 48, pp. 25509-25526, 2022, doi: 10.1039/d2ta07353f.

[17] M. S. Irshad, N. Arshad, J. Zhang, C. Song, N. Mushtaq, M. Alomar, T. Shamim, V.-D. Dao, H. Wang, X. Wang, and H. Zhang, "Wormlike Perovskite Oxide Coupled with Phase-Change

Material for All-Weather Solar Evaporation and Thermal Storage Applications," *Advanced Energy and Sustainability Research,* vol. 4, no. 3, p. 2200158, 2023, doi: 10.1002/aesr.202200158.

[18] X. Liu, D. Liu, J. H. Lee, Q. Zheng, X. Du, X. Zhang, H. Xu, Z. Wang, Y. Wu, X. Shen, J. Cui, Y. W. Mai, and J. K. Kim, "Spider-Web-Inspired Stretchable Graphene Woven Fabric for Highly Sensitive, Transparent, Wearable Strain Sensors," *ACS Appl Mater Interfaces,* vol. 11, no. 2, pp. 2282-2294, 2019, doi: 10.1021/acsami.8b18312.

[19] H. Zou, X. Meng, X. Zhao, and J. Qiu, "Hofmeister Effect-Enhanced Hydration Chemistry of Hydrogel for High-Efficiency Solar-Driven Interfacial Desalination," *Adv Mater,* vol. 35, p. e2207262, 2022, doi: 10.1002/adma.202207262.

[20] W. Zhou, C. Zhou, C. Deng, L. Chen, X. Zeng, Y. Zhang, L. Tan, B. Hu, S. Guo, L. Dong, and S. C. Tan, "High-Performance Freshwater Harvesting System by Coupling Solar Desalination and Fog Collection with Hierarchical Porous Microneedle Arrays," *Adv. Funct. Mater.,* vol. 32, no. 28, p. 2113264, 2022, doi: 10.1002/adfm.202113264.

[21] Q. Zhao, J. Liu, Z. Wu, X. Xu, H. Ma, J. Hou, Q. Xu, R. Yang, K. Zhang, M. Zhang, H. Yang, W. Peng, X. Liu, C. Zhang, J. Xu, and B. Lu, "Robust PEDOT:PSS-based hydrogel for highly efficient interfacial solar water purification," *J. Chem. Eng.,* vol. 442, p. 136284, 2022, doi: 10.1016/j.cej.2022.136284.

[22] J. Yuan, X. Lei, C. Yi, H. Jiang, F. Liu, and G. J. Cheng, "3D-printed hierarchical porous cellulose/alginate/carbon black hydrogel for high-efficiency solar steam generation," *J. Chem. Eng.,* vol. 430, p. 132765, 2022, doi: 10.1016/j.cej.2021.132765.

[23] Z. Yu, R. Gu, Y. Zhang, S. Guo, S. Cheng, and S. C. Tan, "High-flux flowing interfacial water evaporation under multiple heating sources enabled by a biohybrid hydrogel," *Nano Energy,* vol. 98, p. 107287, 2022, doi: 10.1016/j.nanoen.2022.107287.

[24] B. Peng, Q. Lyu, Y. Gao, M. Li, G. Xie, Z. Xie, H. Zhang, J. Ren, J. Zhu, L. Zhang, and P. Wang, "Composite Polyelectrolyte Photothermal Hydrogel with Anti-biofouling and Antibacterial Properties for the Real-World Application of Solar Steam Generation," *ACS Appl Mater Interfaces,* vol. 14, no. 14, pp. 16546-16557, 2022, doi: 10.1021/acsami.2c02464.

[25] A. Ni, D. Fu, P. Lin, Y. Xia, D. Pei, X. Han, S. Hua, S. Li, and T. Zhang, "Rapid Fabrication of Porous Photothermal Hydrogel Coating for Efficient Solar-Driven Water Purification," *ACS Appl Mater Interfaces,* vol. 14, no. 39, pp. 44809-44820, 2022, doi: 10.1021/acsami.2c12073.

[26] X. Liu, F. Chen, Y. Li, H. Jiang, D. D. Mishra, F. Yu, Z. Chen, C. Hu, Y. Chen, L. Qu, and W. Zheng, "3D Hydrogel Evaporator with Vertical Radiant Vessels Breaking the Trade-Off between Thermal Localization and Salt Resistance for Solar Desalination of High-Salinity," *Adv Mater,* vol. 34, no. 36, p. e2203137, 2022, doi: 10.1002/adma.202203137.

[27] X. P. Li, X. Li, H. Li, Y. Zhao, J. Wu, S. Yan, and Z. Z. Yu, "Reshapable MXene/Graphene Oxide/Polyaniline Plastic Hybrids with Patternable Surfaces for Highly Efficient Solar-Driven Water Purification," *Adv. Funct. Mater.,* vol. 32, no. 15, p. 2110636, 2021, doi: 10.1002/adfm.202110636.

[28] L. Geng, L. Li, H. Zhang, M. Zhong, P. Mu, and J. Li, "Interfacial solar evaporator synergistic phase change energy storage for all-day steam generation," *J. Mater. Chem. A,* vol. 10, no. 29, pp. 15485-15496, 2022, doi: 10.1039/d2ta04479j.